JOURNAL OF SOLID STATE CHEMISTRY 73, 179–187 (1988)

Diffusion of Oxide Ion Vacancies in Perovskite-Type Oxides

TAKAMASA ISHIGAKI,*,† SHIGERU YAMAUCHI,‡ KOHJI KISHIO, JUNICHIRO MIZUSAKI,§ AND KAZUO FUEKI

Department of Industrial Chemistry, Faculty of Engineering, University of Tokyo, Hongo, Bunkyo-ku, Tokyo 113, Japan

Received February 2, 1987; in revised form July 13, 1987

In order to elucidate the diffusion of oxide ion vacancies in perovskite-type oxides, we determined the tracer diffusion coefficient of oxide ions, D_O^*, in $La_{1-x}Sr_xCoO_{3-\delta}$ ($x = 0.1$) and $La_{1-x}Sr_xFeO_{3-\delta}$ ($x = 0.1$, 0.25, and 0.4) single crystals. The correlation factor, f, for a vacancy diffusion mechanism in a perovskite-type anion sublattice was calculated to be $f = 0.69$. Using this value and the nonstoichiometry data, the diffusion coefficient of oxide ion vacancies, D_V, was estimated. It was found that D_V in $La_{1-x}Sr_xMO_{3-\delta}$ (M = Co, Fe) take similar values in their magnitude and activation energy. It was concluded that a point defect model holds for the vacancy diffusion in these oxides. The diffusivity of oxide ions in the perovskite-type oxides was comparable to that in fluorite-type oxides.

1. Introduction

The oxides with perovskite-type and perovskite-related structures have been intensively investigated for applications as electrode materials, oxidation catalysts, disposals of radioactive waste matters, and high T_c superconductors. It has been indicated that these oxides have large oxygen deficiencies, and that the deficiencies are related to their properties. In order to elucidate the behavior of oxide ion vacancies in perovskite-type oxides, $La_{1-x}Sr_xMO_{3-\delta}$ (M = Co, Fe), we have carried out diffusion studies (*1–3*) and thermogravimetric measurements (*4, 5*).

In a point defect model with a vacancy diffusion mechanism the self diffusion coefficient of oxide ions, D_O, is proportional to the vacancy concentration, C_V, and the vacancy diffusion coefficient, D_V (*6*).

$$D_O = D_V (C_V/C_O), \qquad (1)$$

where C_O is the oxide ion concentration.

In the previous papers (*1, 2*), we demonstrated that tracer diffusion coefficient of oxide ions, D_O^*, in $LaCoO_{3-\delta}$ and $LaFeO_{3-\delta}$ is proportional to oxide ion vacancy concentration. It was concluded that the point defect model holds for oxide ion vacancy on these oxides and diffusion proceeds by a

* To whom all correspondence should be addressed.

† Present address: National Institute for Research in Inorganic Materials, Namiki, Tsukuba, Ibaraki 305, Japan.

‡ Present address: Research Institute, National Rehabilitation Center for the Disabled, Namiki, Tokorozawa, Saitama 359, Japan.

§ Present address: Institute of Environmental Science and Technology, Yokohama National University, Tokiwadai, Hodogaya-ku, Yokohama, Kanagawa 240, Japan.

0022-4596/88$3.00

vacancy mechanism. It was also shown that D_V in these oxides take similar values. It should be noted again that this infers that the oxide ion vacancy diffusion is described by a point defect model, although there exists an appreciable nonstoichiometry in the oxides (up to = 1.3×10^{-3} in $LaCoO_{3-\delta}$ and 5.8×10^{-6} in $LaFeO_{3-\delta}$ in the oxygen atmosphere of diffusion measurement) (*4, 5*).

When La in $LaCoO_{3-\delta}$ and $LaFeO_{3-\delta}$ is substituted by Sr, the vacancy concentration increases and highly defective perovskite-type oxide is obtained (*4, 5*). The primary objective of this paper is to find out the validity of point defect model in these highly defective perovskite-type structures. To this end, we have measured the tracer diffusion coefficient of oxide ions in single crystals of $La_{1-x}Sr_xCoO_{3-\delta}$ (x = 0.1) and $La_{1-x}Sr_xFeO_{3-\delta}$ (x = 0.1, 0.25, and 0.4) by the gas phase analysis method and the depth profile measurement. The vacancy diffusion coefficient is determined by using Eq. (1) and the following equation,

$$D_O^* = fD_O, \qquad (2)$$

where f is a correlation factor of diffusion.

2. Experimental

2.1 Material

In the measurement of diffusion coefficient, effects of grain boundaries and microstructures may appreciably affect the results. It is, therefore, favorable to make diffusion experiments on single crystals. We have succeeded in the single crystal growth of both solid solutions $La_{1-x}Sr_xMO_{3-\delta}$ (M = Co, Fe) by a floating zone method (*7*).

As-grown single crystals were annealed in air at 1200–1300°C for 2 days and the specimens were fabricated in spheres of 3–5 mm in diameter and slabs of 0.7–0.8 mm thick. The surfaces of the slabs were finely polished.

2.2 Diffusion Annealing and Measurements

(*a*) *Preannealing.* The annealing of specimens was carried out in the apparatus described elsewhere (*1*). The specimens were preannealed at the same oxygen pressure as that for the succeeding diffusion anneal. The purpose of the preannealing is to equilibrate the defect concentration with the desired oxygen partial pressure and to eliminate the surface damage formed during cutting and polishing procedures.

(*b*) *Gas phase analysis method.* Spherical specimens were annealed in an ^{18}O 73.5% enriched oxygen gas (Prochem, Cat. No. OO-409, B. O. C. Limited, UK), and the decrease in $^{18}O/^{16}O$ ratio was monitored by a mass spectrometer. The details were previously given (*1*).

(*c*) *Depth profile measurement.* Slab specimens were annealed in an ^{18}O-enriched oxygen gas for a predetermined time and the ^{18}O depth profile was measured by a secondary ion mass spectrometer (SIMS) (IMA-IIAH, Hitachi, Tokyo). Using the sample with a uniform concentration of 4.2% ^{18}O, the intensity of mass spectra was calibrated *in situ* on every measurement. The depth of an ion-etched crater was measured by a Talystep profilometer. The detailed description on the secondary ion mass spectrometry is given elsewhere (*8*).

3. Results and Discussion

3.1 Gas Phase Analysis Method

The ratio of the diffused amounts of ^{18}O into specimens, M_t/M_∞, were determined by measuring the ratio of isotopic composition of ^{16}O and ^{18}O in the gas phase, where M_t and M_∞ are the total ^{18}O amounts diffusing into the solid for a time t and infinite time, respectively. The observed time dependences of M_t/M_∞ are shown in Figs. 1 and 2. The present experimental condition can be stated by a model of solute diffusing

from a well-stirred solution. The isotopic exchange reaction was affected by surface reaction and it was necessary to analyze the data using the following equations (*9*),

$$\frac{M_t}{M_\infty} = 1 - \sum_{n=1}^{\infty} \frac{6\alpha M^2 (1 + \alpha)}{\alpha^2 q_n^4 + \alpha M\{\alpha(M - 1) - 6\} q_n^2 + 9(1 + \alpha) M^2} \exp\left(-\frac{D_O^* q_n^2 t}{a^2}\right) \quad (3)$$

$$\tan q_n = \frac{3Mq_n - \alpha q_n^3}{\alpha q_n^2 (M - 1) + 3M}, \quad (M = ka/D_O^*) \quad (4)$$

where k is the rate constant of surface reaction, α the ratio of oxygen atoms in the gas phase and the solid phase, a the radius of the sphere specimen, q_n the nonzero roots of Eq. (4).

The data shown in Figs. 1 and 2 were fitted to Eq. (3) to determine D_O^* and k by a nonlinear least-squares analysis using SALS program package at the Computer Center of the University of Tokyo. The results of the calculation are shown in Table 1. The solid lines in Figs. 1 and 2 are those calculated utilizing the determined D_O^* and k. Standard deviations, $\sigma(D_O^*)$ and $\sigma(k)$, in D_O^* and k, respectively, are

	$\sigma(D_O^*)$	$\sigma(k)$
$La_{1-x}Sr_xCoO_{3-\delta}$	<10%	~50%
$La_{1-x}Sr_xFeO_{3-\delta}$	10–25%	10–20%.

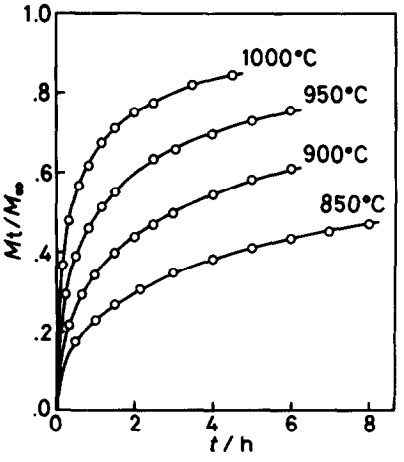

FIG. 1. Diffused amounts of oxygen against time in the gas phase analysis method for $La_{0.9}Sr_{0.1}CoO_{3-\delta}$: $P(O_2)$ = 4.5 kPa.

TABLE I

TRACER DIFFUSION COEFFICIENT OF OXIDE IONS, D_O^*, AND DIFFUSION COEFFICIENT OF OXIDE ION VACANCIES, D_V, BY THE GAS PHASE ANALYSIS METHOD

t (°C)	D_O^* (cm² sec⁻¹)	k (cm sec⁻¹)	Cv[a] (mole)	D_V (cm² sec⁻¹)
$La_{0.9}Sr_{0.1}CoO_{3-\delta}$; $P(O_2)$ = 4.5 kPa				
1000	2.05×10^{-8}	2.31×10^{-6}	9.12×10^{-3}	9.76×10^{-6}
950	7.60×10^{-9}	2.39×10^{-6}	4.37×10^{-3}	7.56×10^{-6}
900	2.61×10^{-9}	1.18×10^{-6}	2.04×10^{-3}	5.55×10^{-6}
850	8.99×10^{-10}	7.81×10^{-7}	9.12×10^{-4}	4.28×10^{-6}
$La_{1-x}Sr_xFeO_{3-\delta}$; $P(O_2)$ = 6.5 kPa				
0.1 1100	2.86×10^{-8}	8.15×10^{-6}	1.11×10^{-2}	1.12×10^{-5}
1050	2.34×10^{-8}	3.62×10^{-6}	8.40×10^{-3}	1.21×10^{-5}
	1.55×10^{-8}	1.27×10^{-6}		8.02×10^{-6}
1000	1.10×10^{-8}	1.85×10^{-6}	6.44×10^{-3}	7.41×10^{-6}
950	4.89×10^{-9}	1.01×10^{-6}	4.63×10^{-3}	4.59×10^{-6}
900	3.22×10^{-9}	5.28×10^{-7}	3.12×10^{-3}	4.49×10^{-6}
	2.31×10^{-9}	6.40×10^{-7}		3.22×10^{-6}
0.25 1050	2.70×10^{-7}	1.03×10^{-5}	4.98×10^{-2}	2.36×10^{-5}
1000	1.25×10^{-7}	4.06×10^{-6}	4.12×10^{-2}	1.32×10^{-5}
950	6.70×10^{-8}	3.08×10^{-6}	3.25×10^{-2}	6.18×10^{-6}
900	3.37×10^{-8}	1.04×10^{-6}	2.41×10^{-2}	6.08×10^{-6}
0.4 1000	5.88×10^{-7}	1.21×10^{-5}	1.31×10^{-1}	1.95×10^{-5}

[a] Determined by thermogravimetry (*4*, *5*).

3.2 Depth Profile Measurement

The depth profile measurements were carried out on $La_{0.9}Sr_{0.1}CoO_{3-\delta}$ at 850 and 800°C and $La_{0.9}Sr_{0.1}FeO_{3-\delta}$ at 900 and 850°C. The ^{18}O depth profiles obtained by SIMS are given in Fig. 3. As is shown in the figure, the ^{18}O concentrations at surfaces are much less than that in the gas phase, 73.5%. This indicates that the isotopic exchange is largely affected by the surface exchange reaction.

The solution of the diffusion equation for the present boundary condition is represented as follows (*10*):

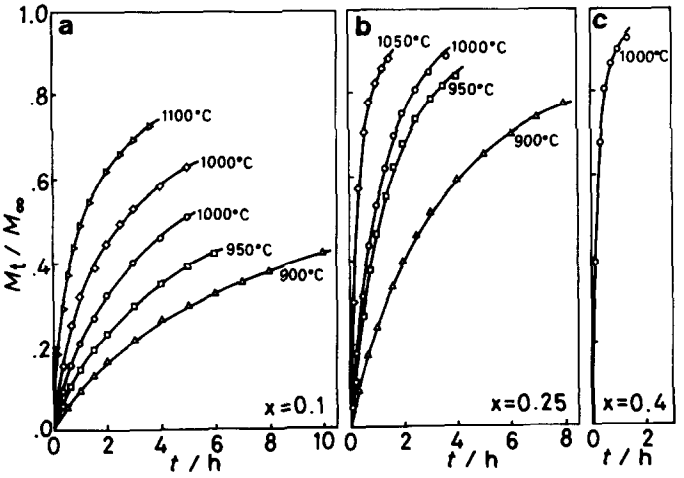

FIG. 2. Diffused amounts of oxygen against time in the gas phase analysis method for $La_{1-x}Sr_xFeO_{3-\delta}$: $P(O_2)$ = 6.5 kPa. (a) x = 0.1; (b) x = 0.25; (c) x = 0.4.

$$\frac{C(x) - C_0}{C_g - C_0} = \mathrm{erfc}\left(\frac{x}{2\sqrt{D_O^* t}}\right) - \exp(hx + h^2 D_O^* t)\,\mathrm{erfc}\left(\frac{x}{2\sqrt{D_O^* t}} + h\sqrt{D_O^* t}\right), \quad (h = k/D_O^*) \quad (5)$$

where $C(x)$ is the ^{18}O concentration of a distance x from the surface for a diffusion time t and C_0 the natural abundance of ^{18}O, 0.204%.

We have previously determined D_O^* and k by fitting the depth profile data to Eq. (5) by a least-squares analysis (*2, 3*). However, it is difficult to analyze the data in Fig. 4, where profiles have very low ^{18}O concentrations at the surface with a linear dependence of a small slope. The slope of the depth profile for a longer annealing time was too small to determine D_O^*. The shortest time that we could control accurately with our heating apparatus was 10 min. Therefore, we had to treat the profile data of 10-min annealing. For a similar depth profile data, Tannhauser and his co-investigators (*11*) have tried a method to estimate the rough value of D_O^*. We have treated the depth profile data carefully to determine the more precise values of D_O^* and k (*7*). The estimated errors in D_O^* and k are 10–20%. The results are given in Table 2.

3.3 Tracer Diffusion Coefficient

In Fig. 4, the tracer diffusion coefficient of oxide ions determined in this work are shown. D_O^* in $LaCoO_{3-\delta}$ (*1*), $LaFeO_{3-\delta}$ (*2*), and $CSZ(Zr_{0.858}Ca_{0.142}O_{1.858})$ (*12*) are also shown for comparison.

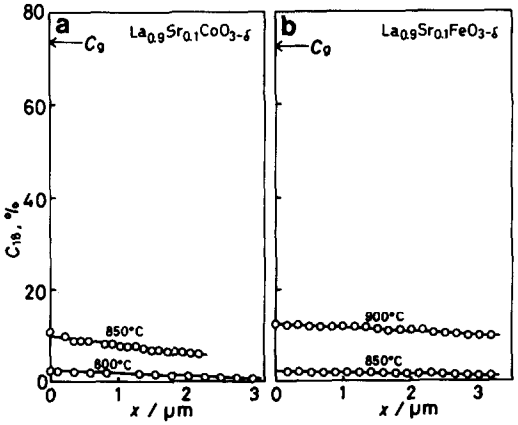

FIG. 3. Concentration profiles of ^{18}O obtained by SIMS. (a) $La_{0.9}Sr_{0.1}CoO_{3-\delta}$: $P(O_2)$ = 4.5 kPa; annealing time = 10 min. (b) $La_{0.9}Sr_{0.1}FeO_{3-\delta}$: $P(O_2)$ = 6.5 kPa; annealing time = 10 min.

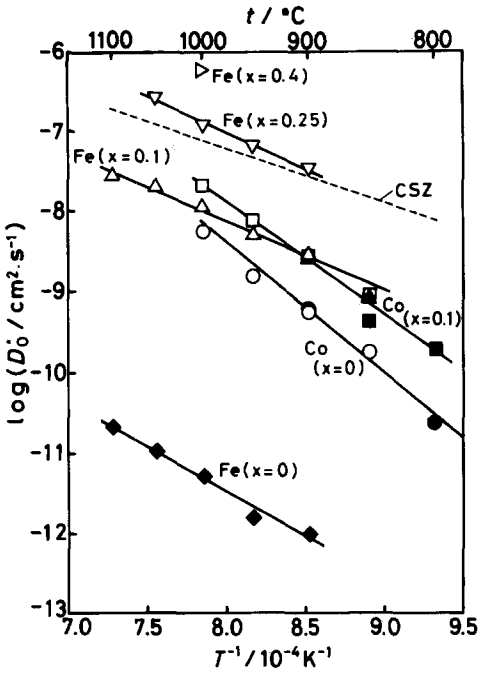

FIG. 4. Tracer diffusion coefficient of oxide ions, D_O^*, in $La_{1-x}Sr_xCoO_{3-\delta}$ [$x = 0$ (○, ●), $x = 0.1$ (□, ■)] and $La_{1-x}Sr_xFeO_{3-\delta}$ [$x = 0$ (◆), $x = 0.1$ (△, ▲), $x = 0.25$ (▽), $x = 0.4$ (▷)]. Open and solid symbols denote D_O^* determined by the gas phase analysis method and that by the depth profile measurement, respectively. For comparison, D_O^* in $CSZ(Zr_{0.858}Ca_{0.142}O_{1.858})$ (*13*) is also shown.

For $La_{0.9}Sr_{0.1}CoO_{3-\delta}$ and $La_{0.9}Sr_{0.1}FeO_{3-\delta}$, D_O^* determined by both methods agree well with each other. This agreement assures that D_O^* can be determined by either method even when an isotopic exchange reaction is affected by a surface reaction.

The temperature dependences of D_O^* in $La_{0.9}Sr_{0.1}CoO_{3-\delta}$ at an oxygen pressure of 4.5 kPa and $La_{1-x}Sr_xFeO_{3-\delta}$ at 6.5 kPa are expressed as follows,

$La_{0.9}Sr_{0.1}CoO_{3-\delta}$:

$$D_O^* = 1.77 \times 10^3 \exp(-(270 \pm 38)\text{kJ mol}^{-1}/RT)\ \text{cm}^2\ \text{sec}^{-1} \quad (6)$$

$La_{1-x}Sr_xFeO_{3-\delta}$

$$x = 0.1\text{: } D_O^* = 5.28 \times 10^{-2} \exp(-(164 \pm 25)\text{kJ mol}^{-1}/RT)\ \text{cm}^2\ \text{sec}^{-1} \quad (7)$$

$$x = 0.25\text{: } D_O^* = 2.45 \times \exp(-(177 \pm 17)\ \text{kJ mol}^{-1}/RT)\ \text{cm}^2\ \text{sec}^{-1}, \quad (8)$$

where the figures after ± denotes 2σ.

The substitution of La^{3+} by Sr^{2+} leads to an increase in D_O^* in both solid solutions. It should be noted that D_O^* in $La_{0.75}Sr_{0.25}FeO_{3-\delta}$ and $La_{0.6}Sr_{0.4}FeO_{3-\delta}$ are comparable to that in CSZ, which is one of the best oxide ion conductors. The activation energies of D_O^* in the oxides including Sr are smaller than that of $LaCoO_{3-\delta}$, 310 kJ mol^{-1} and that of $LaFeO_{3-\delta}$, 214 kJ mol^{-1}, respectively.

In both solid solutions, oxide ions are considered to diffuse via oxide ion vacancies, as in $LaCoO_{3-\delta}$ and $LaFeO_{3-\delta}$. Therefore, the activation energy, Q, of D_O^* is a sum of the formation energy, ΔH_f, and the migration energy, ΔH_m, of oxide ion vacancies (*13*). ΔH_f estimated by utilizing the nonstoichiometric data (*4, 5*) decreases with the increase in Sr content.

$La_{1-x}Sr_xCoO_{3-\delta}$	$x = 0$:	ΔH_f/kJ mol^{-1} = 215
	$x = 0.1$:	184
$La_{1-x}Sr_xFeO_{3-\delta}$	$x = 0$:	137
	$x = 0.1$:	85
	$x = 0.25$:	62.

3.4 Vacancy Diffusion Coefficient

As has been described earlier, the point defect model leads to equation relating tracer diffusion coefficient, D_O^*, and vacancy diffusion coefficient, D_V, by

$$D_O^* = f(C_V/C_O)D_V = f(\delta/(3-\delta))D_V. \quad (9)$$

TABLE II

TRACER DIFFUSION COEFFICIENT OF OXIDE IONS, D_O^*, AND DIFFUSION COEFFICIENT OF OXIDE ION VACANCIES, D_V, BY THE DEPTH PROFILE MEASUREMENT

t (°C)	D_O^* ($cm^2\ sec^{-1}$)	k ($cm\ sec^{-1}$)	Cv[a] (mole)	D_V ($cm^2\ sec^{-1}$)
$La_{0.9}Sr_{0.1}CoO_{3-\delta}$; $P(O_2)$ = 4.5 kPa; annealing time = 10 min				
850	4.34×10^{-10}	1.55×10^{-7}	9.12×10^{-4}	2.07×10^{-6}
800	1.99×10^{-10}	1.54×10^{-8}	3.55×10^{-4}	2.43×10^{-6}
$La_{0.9}Sr_{0.1}FeO_{3-\delta}$; $P(O_2)$ = 6.5 kPa; annealing time = 10 min				
900	2.65×10^{-9}	3.60×10^{-7}	3.12×10^{-3}	3.69×10^{-6}
850	8.51×10^{-10}	2.92×10^{-8}	2.17×10^{-3}	1.70×10^{-6}

[a] Determined by thermogravimetry (*4*, *5*).

The correlation factor, f, of diffusion of oxide ions via vacancies in a perovskite-type oxide has not been reported yet. We applied the resistor lattice method proposed by Compaan and Haven (*14*) to the anion sublattice of a perovskite-type structure and obtained the value of $f = 0.69$. Details are given under Appendix A.

Mizusaki and his co-investigators have determined the nonstoichiometry in the solid solutions by a thermogravimetry (*4*, *5*). They are cited in Tables 1 and 2. The δ increases with the increase in Sr content and that in temperature. $La_{0.6}Sr_{0.4}FeO_{3-\delta}$ has a value as large as 0.131 at 1000°C and 6.5 kPa, which infers that 4.4% of oxide ion lattice is vacant.

The D_V values determined by using Eq. (9) are given in Tables 1 and 2. The temperature dependences of D_V are

$La_{1-x}Sr_xCoO_{3-\delta}$

$x = 0$: $D_V = 2.30 \times 10^{-2}$ exp(−(77 ± 21)kJ mol^{-1}/RT) $cm^2\ sec^{-1}$ (10)

$x = 0.1$: $D_V = 3.92 \times 10^{-2}$ exp(−(79 ± 25)kJ mol^{-1}/RT) $cm^2\ sec^{-1}$ (11)

$La_{1-x}Sr_xFeO_{3-\delta}$

$x = 0$: $D_V = 1.01 \times 10^{-2}$ exp(−(74 ± 24)kJ mol^{-1}/RT) $cm^2\ sec^{-1}$ (12)

$x = 0.1$: $D_V = 1.23 \times 10^{-2}$ exp(−(79 ± 25)kJ mol^{-1}/RT) $cm^2\ sec^{-1}$ (13)

$x = 0.25$: $D_V = 6.83 \times 10^{-2}$ exp(−(114 ± 23)kJ mol^{-1}/RT) $cm^2\ sec^{-1}$ (14)

D_V in $LaCoO_{3-\delta}$ and $LaFeO_{3-\delta}$ have been tentatively reported using the value of $f = 1$ (1, 2) and the present ones are recalculated using $f = 0.69$.

The magnitude of D_V seems almost independent of the Sr content in both solid solutions, although the vacancy concentration increases with the increase in Sr content, and reaches to several percentage of oxide ion sublattice when the Sr content is high.

The activation energy, ΔH_m, of D_V is 75–85 kJ mol^{-1} independent of metal composition, except for $La_{0.75}Sr_{0.25}FeO_{3-\delta}$ with a large value of 114 kJ mol^{-1}. The magnitude of D_V in $La_{0.75}Sr_{0.25}FeO_{3-\delta}$ is similar to those in the other oxides, although some difference is seen in the activation energy. The large activation energy of D_V may be attributed to the comparatively poor accuracy in D_O^*. As is shown by Nanba and his co-investigators (*15*), when the magnitude of D_O^* is relatively large and an isotopic exchange reaction is largely affected by a surface reaction, the accuracy in D_O^* decreases.

Summarizing the above considerations, D_V in $La_{1-x}Sr_xCoO_{3-\delta}$ and $La_{1-x}Sr_xFeO_{3-\delta}$ studied in this work falls in a range of

$$D_V = (1 - 2) \times 10^{-2} \times \exp(-(75 - 85)\text{kJ mol}^{-1}/\text{RT})\ \text{cm}^2\ \text{sec}^{-1}. \quad (15)$$

D_V can also be calculated from the chemical diffusion coefficient, $\tilde{D}$, by the following equation, when the diffusion proceeds by a vacancy mechanism (*16*),

$$\tilde{D} = -\frac{1}{2}\frac{1}{\left(\frac{\partial \ln C_V}{\partial \ln P(O_2)}\right)} D_V. \quad (16)$$

The present results are compared with those calculated from $\tilde{D}$ in $La_{1-x}Sr_xCoO_{3-\delta}$ (x = 0, 0.1) (*3*) in Fig. 5. The agreement between D_V values determined by both methods is excellent and this is considered to prove the vacancy mechanism in a point defect model.

It is noteworthy that D_V remains almost unvaried and it seems that the point defect model still holds even at these high vacancy concentration. This implies that interaction between vacancies is weak in these oxides. It is well known that electronic conductivity in these oxides is very large and in a range of semi-metals (*17*). It is possible that coulombic interactions between ionic defects are shielded by highly populated free electrons.

As is shown under Appendix B, there exists a large discrepancy in the estimated values of D_V in perovskite-type oxides. The reliable defect diffusion coefficients from the data in the literature are those only for fluorite-type oxides.

D_V in fluorite-type oxides are given in Fig. 6. It is found that D_V in the fluorite-type oxides is almost the same and the activation energy of D_V is 45–60 kJ mol^{-1}, irrespective of the method of measurement. In Fig. 6, D_V in perovskite-type oxides obtained in this work are also given. Compared with D_V in fluorite-type oxides, D_V in perovskite-type oxides is nearly the same, although ΔH_m is slightly larger. That is, the diffusivities of oxide ions in both oxides are nearly equal.

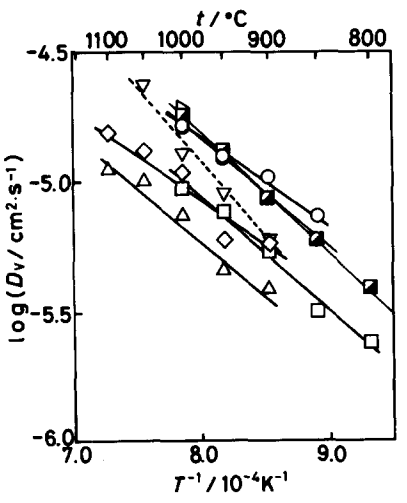

FIG. 5. Diffusion coefficient of oxide ion vacancies, D_V, in $La_{1-x}Sr_xCoO_{3-\delta}$ (x = 0 (○, ◕), 0.1 (□, □)) and $La_{1-x}Sr_xFeO_{3-\delta}$ (x = 0 (◇), 0.1 (△), 0.25 (▽), 0.4 (▷)). Symbols ◕ and ◪ denote D_V derived from $\tilde{D}$ (*3*).

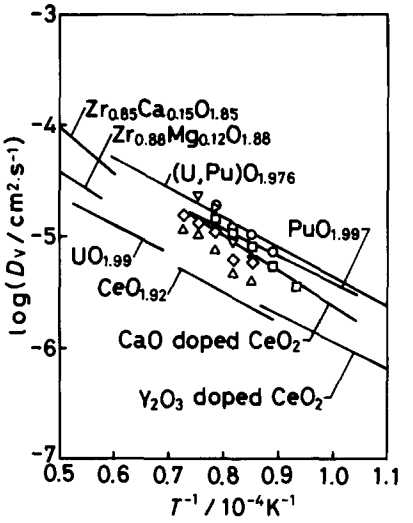

FIG. 6. Comparison of diffusion coefficient of oxide ion vacancies, D_V, between the perovskite-type oxides ($La_{1-x}Sr_xMO_{3-\delta}$; M = Co and Fe) and some fluorite-type oxides; $Zr_{0.88}Mg_{0.12}O_{1.88}(D_O^*)$ (*18*), $Zr_{0.85}Ca_{0.15}O_{1.85}(D_O^*)$ (*18*), $UO_{1.99}(D_O^*)$ (*19*), $(U,Pu)O_{1.976}(\tilde{D})$ (*20*), $PuO_{1.99}(\tilde{D})$ (*21*), $CeO_{1.92}(D_O^*)$ (*22*), CaO doped CeO_2 (σ_O) (*23*), and Y_2O_3 doped CeO_2 (^{17}O NMR, extrapolated from 400 to 110°C) (*24*). Symbols for the perovskite-type oxides are the same as those in Fig. 5.

Appendix A

Using the method proposed by Compaan and Haven (*14*), we calculated the correlation factor of a tracer oxide ion diffusion via vacancies in a perovskite-type oxide.

The correlation factor, f, for a vacancy mechanism is represented by

$$f = \frac{1 + \langle \cos \theta_{i,i+1} \rangle}{1 - \langle \cos \theta_{i,i+1} \rangle}, \qquad \text{(A1)}$$

where $\theta_{i,i+1}$ denotes the angle between two successive jump vectors i and $i+1$, and the brackets denote the averaging overall possibilities. In order to estimate the value of $\langle \cos \theta_{i,i+1} \rangle$, Compaan and Haven (*14*) proposed a calculation method with occupation probability, and the alternative method of a potential measurement using an electrical network of resistors, isomorphous to the crystal lattice.

Although Compaan and Haven actually constructed a resistor network and made the potential measurement, we adopted a purely computational work and simulated the network. Using Kirchihoff's rule, a set of first-order linear equations was determined and directly solved via a matrix calculation.

The results of our calculation gave the values of f, 0.70213, 0.69231, and 0.69117 for the network with the number of steps, 2, 3, and 4, away from the origin, respectively. Compaan and Haven showed that the number of 4 steps seems to be sufficient for a rough estimation. We approximated the value of f as 0.69.

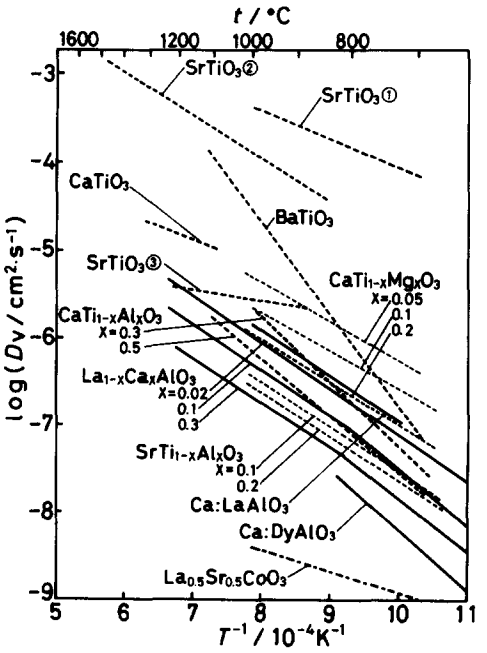

FIG. 7. Diffusion coefficient of oxide ion vacancies, D_V, in some perovskite-type oxides. $La_{1-x}Ca_xAlO_3$ (σ_O) (*25*); Ca : $LaAlO_3(La_{0.95}Ca_{0.05}AlO_3)(\sigma_O)$ (*26*); Ca : $DyAlO_3(Dy_{0.975}Ca_{0.025}AlO_3)(\sigma_O)$ (*26*); $CaTiO_3(\tilde{D})$ (*27*); $SrTiO_3$ ① ($\tilde{D}$) (*28*), ② ($\tilde{D}$) (*29*), ③ ($\tilde{D}$) (*30*); $Ca\,Ti_{1-x}Al_xO_3(\sigma_O)$ (*31*); $CaTi_{1-x}Mg_xO_3(\sigma_O)$ (*32*); $SrTi_{1-x}Al_xO_3(\sigma_O)$ (*33*); $BaTiO_3$ ($\tilde{D}$) (*34*); and $La_{0.5}Sr_{0.5}CoO_3$ ($\tilde{D}$, extrapolated from 100 to 20°C) (*35*).

Appendix B

We tried to elucidate D_V in perovskite-type oxides from the existing data. To this end, the data of the chemical diffusion coefficient and ionic conductivity can be utilized (*25–36*). For the electronic conductors, such as $CaTiO_3$ and $SrTiO_3$, D_V can be calculated by using Eq. (16) ($(\partial \ln C_V / \partial \ln P(O_2)) = -1/6$; $CaTiO_3$ (*37*), $SrTiO_3$ (*38*)). For solid electrolytes, such as $LaAlO_3$, the ionic conductivity of oxide ions, σ_O, has the following relation with D_V using the Nernst–Einstein equation and Eq. (1),

$$\sigma_O = 2^2 F^2 C_V (D_V/RT). \qquad (B1)$$

The vacancy diffusion coefficient calculated by Eqs. (16) and (B1) are represented in Fig. 7. The calculated values are seen to largely scatter in both magnitude and activation energy. A typical example is D_V in titanates. Although many studies have been reported, we could not find a reliable one.

References

1. T. ISHIGAKI, S. YAMAUCHI, J. MIZUSAKI, K. FUEKI, AND H. TAMURA, *J. Solid State Chem.* **54,** 100 (1984).
2. T. ISHIGAKI, S. YAMAUCHI, J. MIZUSAKI, K. FUEKI, H. NAITO, AND T. ADACHI, *J. Solid State Chem.* **55,** 50 (1984).
3. K. FUEKI, J. MIZUSAKI, S. YAMAUCHI, T. ISHIGAKI, AND Y. MIMA, "Proceedings of the 10th International Symposium on Reactivity of Solids, 1984" (P. Barret and L.-C. Dufour, Eds.), p. 339, Elsevier, Amsterdam (1985).

4. J. MIZUSAKI, M. YOSHIHIRO, S. YAMAUCHI, AND K. FUEKI, *J. Solid State Chem.* **58,** 257 (1985).
5. J. MIZUSAKI, Y. MIMA, S. YAMAUCHI, AND K. FUEKI, submitted for publication.
6. H. SCHMALZRIED, "Solid State Reactions," Materials Science Series, p. 56, Verlag Chemie, Weinheim (1974).
7. T. MATSUURA, T. ISHIGAKI, J. MIZUSAKI, S. YAMAUCHI, AND K. FUEKI, *Japan. J. Appl. Phys.* **23,** 1172 (1984).
8. T. ISHIGAKI, S. YAMAUCHI, AND K. FUEKI, *Yogyo-Kyokai-Shi* **95,** 1031 (1987).
9. H. S. EDWARDS, A. F. ROSENBERG, AND J. T. BITTEL, "Report No. ASD-TDR-63-635," Aeronautical Systems Division, Wright-Patterson Air Force Base, OH (1963).
10. J. CRANK, "The Mathematics of Diffusion," 2nd ed., p. 36, Oxford Univ. Press, London (1975).
11. D. S. TANNHAUSER, J. A. KILNER, AND B. C. H. STEELE, *Nucl. Instrum. Methods* **218,** 504 (1983).
12. L. A. SIMPSON AND R. E. CARTER, *J. Amer. Ceram. Soc.* **49,** 139 (1966).
13. P. KOFSTAD, "Nonstoichiometry, Diffusion and Electrical Conductivity in Binary Metal Oxides," p. 80, Wiley, New York (1972).
14. K. COMPAAN AND Y. HAVEN, *Trans. Faraday Soc.* **52,** 786 (1956).
15. M. NANBA, Y. OISHI, AND K. ANDO, *J. Chem. Phys.* **75,** 913 (1981).
16. C. WAGNER, *Z. Phys. Chem. B* **32,** 447 (1936).
17. J. B. GOODENOUGH, *in* "Progress in Solid State Chemistry," (H. Reiss, Eds.), Vol. 5, p. 145, Pergamon, New York (1967).
18. Y. OISHI, K. ANDO, AND M. AKIYAMA, *Nippon Kagaku Kaishi* **1981,** 1445.
19. K. C. KIM AND D. R. OLANDER, *J. Nucl. Mater.* **102,** 192 (1981).
20. A. S. BAYOGLU AND R. LORENZELLI, *J. Nucl. Mater.* **79,** 437 (1979).
21. A. S. BAYOGLU AND R. LORENZELLI, *J. Nucl. Mater.* **82,** 403 (1979).
22. B. C. H. STEELE AND J. M. FLOYD, *Proc. Brit. Ceram. Soc.* **19,** 55 (1971).
23. R. N. BLUMENTAL, F. S. BRUGER, AND J. E. GARNIER, *J. Electrochem. Soc.* **120,** 1230 (1973).
24. K. FUDA, K. KISHIO, S. YAMAUCHI, K. FUEKI, AND Y. ONODA, *J. Phys. Chem. Solids* **45,** 1253 (1984).
25. H. IWAHARA AND T. TAKAHASHI, *Denki Kagaku* **35,** 433 (1967).
26. J. A. KILNER AND R. J. BROOK, *Solid State Ionics* **6,** 237 (1982).
27. W. L. GEORGE AND R. E. GRACE, *J. Phys. Chem. Solids* **30,** 889 (1969).
28. D. B. SCHWARZ AND H. V. ANDERSON, *J. Electrochem. Soc.* **122,** 707 (1975).
29. A. E. PALADINO, *J. Amer. Ceram. Soc.* **48,** 476 (1965).
30. L. C. WALTERS AND R. E. GRACE, *J. Phys. Chem. Solids* **28,** 245 (1967).
31. H. IWAHARA AND T. TAKAHASHI, *Denki Kagaku* **39,** 400 (1971).
32. T. TAKAHASHI AND H. IWAHARA, *Energy Convers.* **11,** 105 (1971).
33. T. TAKAHASHI, H. IWAHARA, AND T. ICHIMURA, *Denki Kagaku* **37,** 857 (1969).
35. F. R. VAN BUREN, G. H. J. BROERS, A. J. BOUMAN, AND C. BOESVELD, *J. Electroanal. Chem.* **88,** 353 (1978).
36. R. WERNICKE, *Philips Res. Rep.* **31,** 526 (1976).
37. N. G. EROR AND V. BALACHANDRAN, *J. Solid State Chem.* **43,** 196 (1982).
38. V. BALACHANDRAN AND N. G. EROR, *J. Mater. Sci.* **17,** 2133 (1982).